MATERIALE PLASTICE
https://revmaterialeplastice.ro
https://doi.org/10.37358/Mat.Plast.1964

In Vitro Evaluation of Thermosensitive PLGA–PEG–PLGA Hydrogels for Sustained Dexamethasone Delivery and Anti-Inflammatory Effects in Prostate Epithelial Cells

CHENGLONG ZHENG[1], HUIQING WU[2], HUI WANG[3]*, YUE LAN[4]*
[1] Department of Andrology, Dongfang Hospital, Beijing University of Chinese Medicine, Beijing, China
[2] Department of Laboratory Medicine, Gulou Hospital of Traditional Chinese Medicline, Beijing, China
[3] Department of Internal Medicine, The Hospital of Traditional Chinese Medicine Chaoyang District, Beijing, China
[4] Department of Traditional Chinese Medicine, Fuwai Hospital, Chinese Academy of Medical Sciences, Beijing, China

Abstract: ***Background*****:** *Thermosensitive hydrogels have been widely investigated for localized drug delivery; however, their in vitro physicochemical stability, degradation behavior, and cell-level anti-inflammatory performance require systematic evaluation before further translational studies. In particular, prostate epithelial inflammation remains an underexplored application scenario for such delivery platforms.* ***Methods*****:** *In this study, a PLGA–PEG–PLGA thermosensitive hydrogel was evaluated as a sustained delivery system for dexamethasone. The copolymer was characterized by GPC, FTIR, and* ^{1}*H NMR. Sol–gel transition behavior and viscoelastic properties were assessed using micro-DSC and rheological analysis. The microstructure of the drug-loaded hydrogel was examined by SEM. Degradation behavior was investigated under physiological (PBS, 37°C) and accelerated alkaline conditions. Cytocompatibility and anti-inflammatory effects were evaluated in RWPE-1 prostate epithelial cells.* ***Results*****:** *SEM revealed an interconnected porous network structure in the drug-loaded hydrogel. Degradation studies showed high structural stability in PBS with minimal mass loss over 14 days, while rapid degradation occurred under alkaline conditions, confirming hydrolytic degradability. The hydrogel enabled sustained dexamethasone release and maintained good cytocompatibility. Notably, dexamethasone-loaded hydrogels significantly reduced IL-6 and IL-8 secretion, whereas blank hydrogels showed no intrinsic anti-inflammatory effect.* ***Conclusion*****:** *This work provides a comprehensive in vitro evaluation of a thermosensitive PLGA–PEG–PLGA hydrogel for sustained dexamethasone delivery at the cellular level. The results clarify the relationship between hydrogel microstructure, degradation behavior, and diffusion-dominated drug release, establishing a solid foundation for future in vivo investigations.*

Keywords: *PLGA–PEG–PLGA, thermosensitive hydrogel, dexamethasone, localized drug delivery, prostatitis, sustained release, anti-inflammatory therapy*

1. Introduction

Chronic prostatitis/chronic pelvic pain syndrome (CP/CPPS) is one of the most prevalent urological disorders in men, characterized by recurrent pelvic pain, urinary dysfunction, and compromised quality of life [1,2]. Despite its high incidence and substantial socioeconomic burden, the pathogenesis of CP/CPPS remains multifactorial and incompletely understood, involving persistent inflammation, infection, and immune dysregulation [3,4]. Current treatment strategies, including oral antibiotics, anti-inflammatory agents, and α-blockers, often exhibit unsatisfactory efficacy due to poor drug penetration into the prostate tissue, rapid systemic clearance, and dose-limiting side effects [5]. Therefore, there is an urgent need to develop new therapeutic modalities capable of achieving localized, sustained, and effective drug delivery to the prostate [6,7].

**email: 20180941047@bucm.edu.cn, ly229257613@163.com*

Hydrogel-based drug delivery systems have attracted growing attention as injectable carriers for local therapy owing to their high-water content, tunable mechanical properties, and ability to encapsulate a wide range of bioactive molecules [8,9]. In particular, thermosensitive hydrogels are of great interest because they undergo a sol–gel phase transition in response to physiological temperature [10]. This property enables minimally invasive administration as a free-flowing solution at low temperature and rapid *in situ* gelation upon injection, thereby forming a depot that provides controlled drug release at the target site [11]. Such systems have been widely explored in cancer therapy, wound healing, and tissue regeneration, yet their potential in the context of prostatitis treatment remains underexplored [12,13].

Among thermosensitive hydrogel candidates, PLGA–PEG–PLGA triblock copolymers stand out due to their excellent biocompatibility, biodegradability, and well-defined sol–gel transition behavior near body temperature [14,15]. The amphiphilic structure drives self-assembly into micelles and subsequent gelation via physical crosslinking, without requiring toxic chemical crosslinkers [16,17]. Importantly, the hydrophilic–hydrophobic balance of the copolymer can be finely tuned to optimize gelation temperature, mechanical stability, and drug release kinetics [18]. These features make PLGA–PEG–PLGA hydrogels highly suitable for localized delivery of anti-inflammatory drugs in the prostate microenvironment [19,20]. Although PLGA–PEG–PLGA hydrogels have been previously applied in several inflammatory and regenerative contexts, their use in prostate-related inflammation remains largely unexplored. Chronic prostatitis presents distinct therapeutic challenges, including limited drug penetration into the prostate epithelium and persistent cytokine dysregulation, making it a biologically relevant but understudied application scenario. In this work, the innovation lies in establishing an integrated *in vitro* platform that combines thermoresponsive injectability, controlled dexamethasone release, and cytokine suppression specifically in RWPE-1 prostate epithelial cells. This model enables mechanistic evaluation of hydrogel-mediated anti-inflammatory effects within a prostate-relevant cellular environment. Furthermore, dexamethasone was selected as the representative drug due to its established clinical use for inflammation management and its well-defined glucocorticoid signaling pathway, allowing clear interpretation of cytokine modulation. By focusing on a single, well-characterized formulation, our study provides foundational insight into how a thermosensitive PLGA–PEG–PLGA hydrogel may modulate inflammatory responses in prostate epithelial cells, thereby differentiating this work from prior applications in other tissues.

Dexamethasone, a potent glucocorticoid, has been extensively used for its anti-inflammatory and immunosuppressive effects [21,22]. However, systemic administration of dexamethasone is associated with multiple side effects, including metabolic disturbances and immunosuppression, which limit its long-term use [23]. Localized delivery of dexamethasone using an injectable hydrogel system may overcome these limitations by reducing systemic exposure, prolonging drug retention in the prostate, and achieving sustained anti-inflammatory efficacy [24].

In this study, we designed and evaluated a thermosensitive PLGA–PEG–PLGA hydrogel system for localized delivery of dexamethasone in the treatment of prostatitis. The copolymer was synthesized and structurally characterized by GPC, FTIR, and ^{1}H NMR. The sol–gel transition behavior was systematically investigated by DSC and rheological measurements, and injectability was assessed under clinically relevant conditions. *In vitro* drug release experiments were conducted to compare hydrogel-encapsulated dexamethasone with free drug. Furthermore, cytocompatibility, cell morphology, and anti-inflammatory efficacy were examined using prostate epithelial cells. Collectively, these results aim to demonstrate that PLGA–PEG–PLGA hydrogel provides a promising minimally invasive platform that integrates controlled release, favorable biocompatibility, and anti-inflammatory function for the localized treatment of prostatitis.

2. Materials and Methods

Poly(ethylene glycol) (PEG, Mn ≈ 1500, Cat# 202468), L-lactide (LA, Cat# L1750), and glycolide (GA, Cat# 276245) were purchased from Sigma–Aldrich (St. Louis, MO, USA). Stannous octoate

($Sn(Oct)_2$, Cat# S3252) was obtained from Sigma–Aldrich. Dexamethasone (Cat# D4902) was purchased from Aladdin Biochemical Technology Co., Ltd. (Shanghai, China). Dulbecco's modified Eagle medium (DMEM, Cat# 11965-092), fetal bovine serum (FBS, Cat# 10099-141), penicillin–streptomycin (Cat# 15140-122), and CCK-8 kit (Cat# CK04) were purchased from Gibco, Thermo Fisher Scientific (Waltham, MA, USA). Phalloidin–FITC (Cat# A12379) and DAPI (Cat# D1306) were obtained from Invitrogen (Carlsbad, CA, USA). Human cervical carcinoma cells (RWPE-1) were purchased from Cell Bank of Chinese Academy of Sciences (Shanghai, China). Human IL-6 ELISA kit (Cat# ab178013) and IL-8 ELISA kit (Cat# ab214030) were purchased from Abcam (Cambridge, UK). All reagents were of analytical grade and used as received unless otherwise noted. Ultrapure water was prepared using a Milli-Q purification system (Millipore, Burlington, MA, USA).

2.1. Synthesis of PLGA–PEG–PLGA triblock copolymer

The triblock copolymer PLGA–PEG–PLGA was synthesized by ring-opening polymerization. Briefly, PEG (5 g, dried under vacuum at 80°C for 12 h) was introduced into a dry round-bottom flask, followed by the addition of LA and GA at a feed molar ratio of 10:1. Stannous octoate (0.05% w/w of monomers) was added as the catalyst. The reaction was performed under nitrogen atmosphere at 140°C for 24 h with continuous stirring. After cooling to room temperature, the product was dissolved in dichloromethane, precipitated in cold diethyl ether, and dried under vacuum. The copolymer was stored at −20°C until further use.

2.2. Characterization

Gel permeation chromatography (GPC): Molecular weight and distribution were measured using a Waters GPC system (Waters 2414, USA) with THF as eluent at 35°C, calibrated against polystyrene standards.

Fourier transform infrared spectroscopy (FTIR): FTIR spectra were recorded on a Nicolet iS50 spectrometer (Thermo Fisher, USA) in the range 4000–500 cm^{-1} using KBr pellets.

^1H NMR spectroscopy: ^1H NMR spectra were obtained using a Bruker AVANCE 400 MHz spectrometer (Bruker, Germany) with $CDCl_3$ as solvent and TMS as internal standard.

Scanning electron microscopy (SEM): The microstructure of the dexamethasone-loaded PLGA–PEG–PLGA hydrogel was examined by scanning electron microscopy. Briefly, hydrogels were prepared at the designed polymer concentration and incubated at 37°C until complete gelation. The samples were then frozen at −80°C for at least 12 h and lyophilized (freeze-dried) to obtain dry porous scaffolds. The lyophilized hydrogels were fractured to expose internal cross-sections (liquid nitrogen fracturing was used when necessary to obtain a clean brittle surface). The specimens were mounted on aluminum stubs using conductive carbon tape and sputter-coated with a thin gold (or gold/palladium) layer (~5–10 nm) to prevent charging.

2.3. Differential scanning calorimetry (DSC)

Thermal transition behavior was analyzed using a Micro-DSC III (Setaram, France). Samples (10 mg) were sealed in aluminum pans and heated from 10°C to 90°C at 2°C/min under nitrogen. The sol–gel transition temperature was determined from the peak of the endothermic transition.

2.4. Rheological measurements

Rheological properties were assessed using a stress-controlled rheometer (TA Instruments AR2000, USA) with a parallel plate geometry (diameter 40 mm, gap 0.5 mm).

Temperature sweep: Hydrogel solutions (20 wt%) were subjected to oscillatory shear at a fixed frequency of 1 Hz and strain of 1% while heating from 10°C to 45°C at 1°C/min. Storage modulus (G') and loss modulus (G'') were recorded.

Frequency sweep: Measurements were performed at 37°C over an angular frequency range of 0.1–100 rad/s with constant strain (1%).

2.5. Injectability test

Injectability was evaluated using a universal testing machine (Instron 3343, Norwood, MA, USA). Hydrogel solutions (20 wt%) were loaded into 2 mL syringes and extruded through 22G, 23G, or 25G needles at injection rates of 1 or 3 mL/min. The force–displacement curves were recorded, and peak injection force was analyzed.

2.6. In vitro degradation of hydrogel and drug release study

In vitro degradation of the dexamethasone-loaded PLGA–PEG–PLGA hydrogel was evaluated by monitoring the remaining mass over time under physiological and accelerated conditions. Hydrogels were cast into cylindrical molds (diameter 10 mm, thickness 1 mm) and allowed to fully gel at 37°C. Each sample was then lyophilized to a constant weight and recorded as the initial dry mass (W_0). The specimens were immersed in (i) PBS (pH 7.4) at 37°C to simulate physiological conditions, or (ii) 0.5 M NaOH at 37°C as an accelerated hydrolysis condition. For each sample, a fixed medium volume was used (10 mL per specimen) in sealed tubes, and the media were refreshed daily to maintain sink conditions. At predetermined time points (daily from day 0 to day 14), samples were removed, gently rinsed with deionized water to remove residual salts, blotted to remove surface liquid, frozen at −80°C, and lyophilized to constant weight to obtain the remaining dry mass.

Dexamethasone-loaded hydrogel (equivalent to 1 mg drug) was placed in a dialysis bag (MWCO3.5 kDa, Thermo Fisher, Cat# 88245) and immersed in 20 mL phosphate-buffered saline (PBS, pH 7.4) at 37°C under shaking (100 rpm). At predetermined intervals, 1 mL of release medium was collected and replaced with fresh PBS. Drug concentrations were determined by UV–vis spectrophotometry at 242 nm (UV-2600, Shimadzu, Japan). Release profiles were plotted as cumulative release percentage vs. time.

2.7. Cell culture and viability assay

RWPE-1 cells were cultured in DMEM supplemented with 10% FBS and 1% penicillin–streptomycin at 37°C in a humidified 5% CO_2 incubator. For CCK-8 assay, cells were seeded in 96-well plates at 5×10^3 cells/well and treated with hydrogel extracts (prepared by incubating 200 mg hydrogel in 1 mL culture medium for 24 h) for 24 and 72 h. At each time point, 10 µL CCK-8 reagent was added per well, incubated for 2 h, and absorbance was measured at 450 nm using a microplate reader (BioTek Synergy H1, USA). Cell viability was normalized to untreated controls.

2.8. Cytoskeleton staining and image analysis

Cells were seeded on coverslips in 24-well plates and treated with hydrogel extracts for 24 h. After fixation with 4% paraformaldehyde (Cat# P1110, Solarbio, Beijing, China) for 15 min and permeabilization with 0.1% Triton X-100 for 5 min, cells were stained with Phalloidin–FITC (5 µg/mL, 30 min) and counterstained with DAPI (1 µg/mL, 5 min). Fluorescence images were acquired with a confocal microscope (Leica TCS SP8, Germany). Cell area and spreading index were quantified using ImageJ software (NIH, USA).

2.9. ELISA assay

To evaluate inflammatory cytokine secretion, RWPE-1 cells were seeded in 6-well plates (2×10^5 cells/well) and treated with hydrogel extracts for 24 h. The supernatants were collected and analyzed for IL-6 and IL-8 levels using human ELISA kits (Abcam, UK) according to the manufacturer's instructions. Absorbance was measured at 450 nm using a microplate reader (BioTek Synergy H1, USA).

3. Results

As shown in Figure 1, the PLGA–PEG–PLGA triblock copolymer exhibited a distinct temperature-sensitive sol–gel transition. At low temperature, the copolymer solution remained in a free-flowing state, allowing for facile syringe injection. Upon warming to body temperature, the polymer chains

underwent self-assembly into micellar structures, leading to rapid gelation and the formation of a stable hydrogel depot. This transition was accompanied by the entrapment of dispersed therapeutic molecules within the gel matrix. Furthermore, local injection into the prostatic region enabled the hydrogel to conform to the tissue environment and establish a sustained drug reservoir. The lower panel of Figure 1 demonstrates that drug molecules were initially confined within the hydrophilic domains of the micelles and subsequently released through a diffusion-dominated process. Over time, the network gradually loosened, facilitating continuous and extended release of the encapsulated drug. Together, these results indicate that the thermoresponsive hydrogel system is capable of minimally invasive administration and controlled release within the prostate microenvironment.

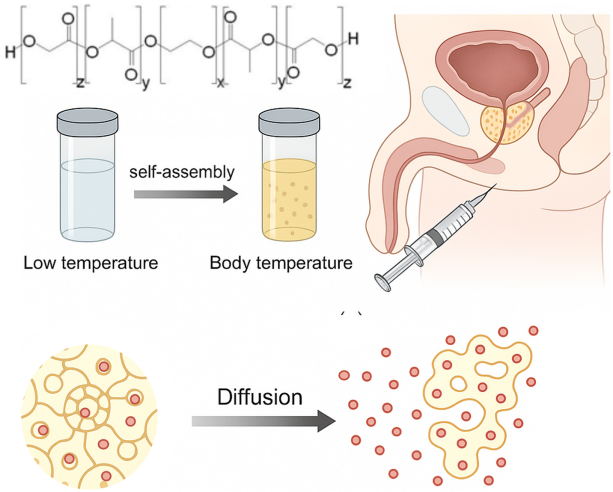

Figure 1. Schematic illustration of the thermosensitive PLGA–PEG–PLGA hydrogel for local drug delivery in prostatitis therapy. The triblock copolymer remains a free-flowing solution at low temperature and undergoes sol–gel transition upon exposure to body temperature through self-assembly of micellar structures. Following intraprostatic injection, the hydrogel forms an *in-situ* depot that encapsulates therapeutic molecules. Drug release occurs gradually via diffusion through the micellar network, providing sustained and localized delivery to the prostate microenvironment

As shown in Figure 2A, the GPC analysis revealed a single sharp elution peak without secondary shoulders, indicating uniform polymerization and absence of significant degradation products. The FTIR spectrum (Figure 2B) displayed characteristic absorption peaks attributable to C=O stretching, C–O–C stretching, and methylene groups, confirming the successful incorporation of PEG and PLGA segments. In the ^{1}H NMR spectrum (Figure 2C), the integration of PEG (δ~3.64 ppm), LA (δ~5.2 ppm), and GA (δ~4.8 ppm) resonances yielded PEG:LA $\approx$ 9:1 and LA:GA $\approx$ 1.5:1, values closely matching the theoretical feed ratios. These results collectively demonstrate the successful synthesis of the intended PLGA–PEG–PLGA copolymer with well-defined composition.

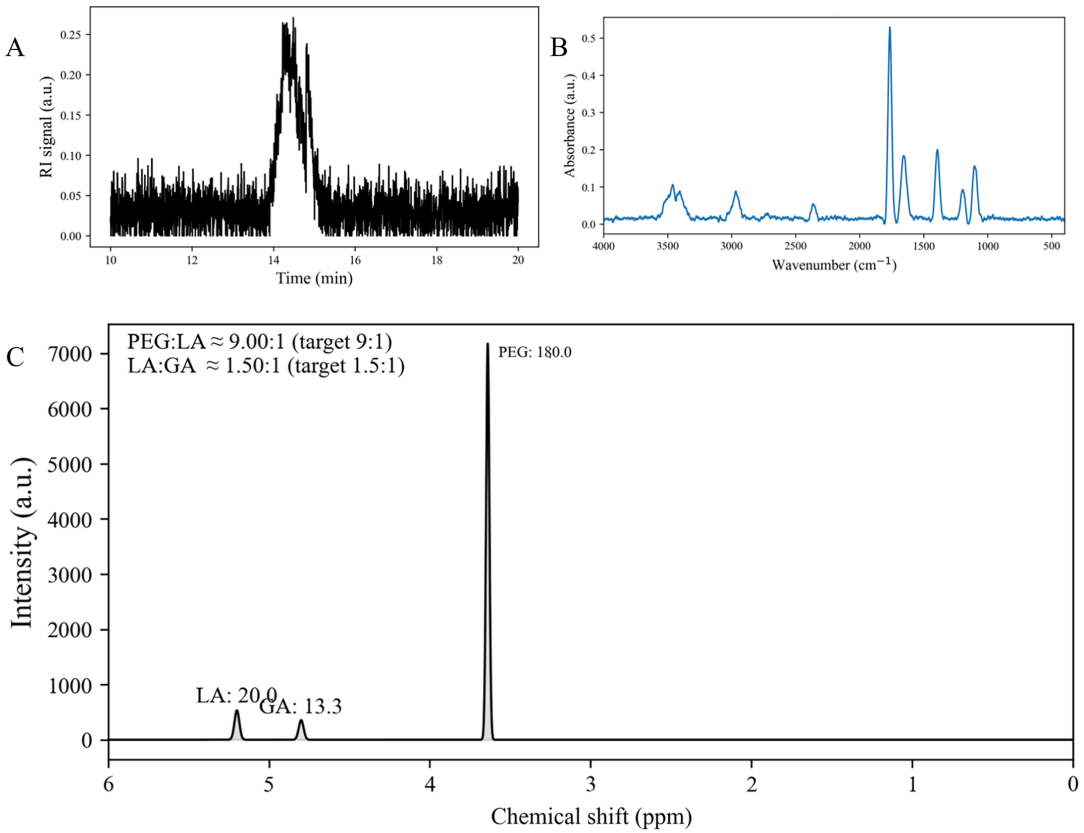

Figure 2. Characterization of the PLGA–PEG–PLGA copolymer. (A) GPC chromatogram showing a unimodal peak, indicative of narrow molecular weight distribution. (B) FTIR spectrum confirming the presence of characteristic functional groups of PEG and PLGA segments. (C) ^{1}H NMR spectrum used to calculate block ratios, showing integral values corresponding to PEG, LA, and GA units with PEG:LA ≈ 9:1 and LA:GA ≈ 1.5:1, consistent with the targeted feed ratio

Figure 3 illustrates the typical sol–gel transition and mechanical characteristics of the PLGA–PEG–PLGA formulation. The vial-inversion test confirmed that the solution remained fluid at low temperature but transformed into a non-flowing gel at body temperature. Calorimetric analysis detected a pronounced endothermic peak at ~33°C, consistent with the expected micellization-driven gelation process. Rheological measurements further validated the thermoresponsive transition: the storage modulus (G′) overtook the loss modulus (G″) near 32.6°C, signifying the formation of an elastic gel network. At 37°C, frequency sweep analysis demonstrated a crossover point at ~3.7 rad/s, indicating frequency-dependent viscoelasticity typical of physically crosslinked hydrogels. In addition, injection force measurements under various needle sizes and flow rates showed that the hydrogel could be readily extruded through clinically relevant needles, with forces remaining within an acceptable range even at higher rates.

Figure 4 summarizes the *in vitro* release and cellular responses to the hydrogel system. The release study revealed that dexamethasone encapsulated in PLGA–PEG–PLGA gel exhibited a sustained and gradual release profile, while free drug diffused rapidly within the first 12 h before reaching plateau. CCK-8 assays demonstrated that cells cultured with the hydrogel maintained comparable or even slightly enhanced viability compared with control groups, particularly at 72 h. The ELISA results revealed clear differences among the three treatment groups. As expected, the blank PLGA–PEG–PLGA hydrogel did not significantly affect IL-6 or IL-8 secretion compared with the untreated control, indicating that the polymer matrix itself does not exert an intrinsic anti-inflammatory effect. In contrast, cells treated

with the dexamethasone-loaded hydrogel exhibited a pronounced reduction in both cytokines. These data demonstrate that the observed anti-inflammatory response is primarily attributable to the sustained release of dexamethasone rather than to the hydrogel material alone.

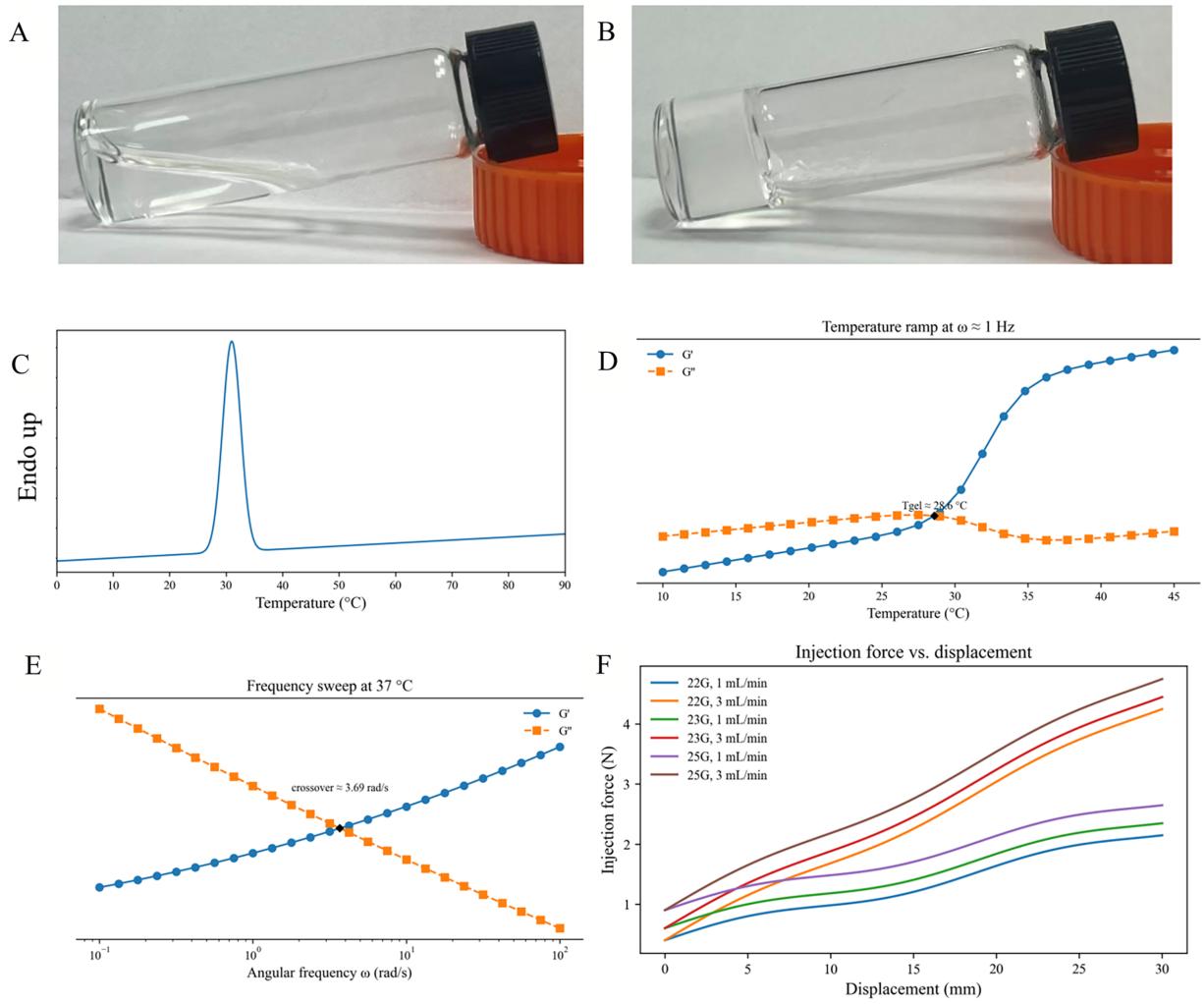

Figure 3. Thermoresponsive behavior, rheological properties, and injectability of the PLGA–PEG–PLGA hydrogel. (A,B) Photographs demonstrate the sol state at low temperature and gel formation at body temperature. (C) μDSC thermogram reveals a sharp endothermic transition around 32°C–34°C. (D) Temperature sweep rheology confirms sol–gel transition, where G′ surpasses G″ at ~32.6°C. (E) Frequency sweep at 37°C shows a crossover of G′ and G″ at ~3.7 rad/s, indicating a viscoelastic gel network. (F) Injection force–displacement curves under different needle gauges and injection rates highlight the practical injectability of the hydrogel system

The microstructure of the dexamethasone-loaded PLGA–PEG–PLGA hydrogel was examined by SEM. As shown in Figure 5, the freeze-dried hydrogel exhibited an interconnected porous network with irregular pore shapes and rough pore walls, indicating the formation of a physically crosslinked three-dimensional structure. After degradation treatment, the hydrogel surface became denser and less porous, suggesting gradual network collapse and polymer erosion.

The degradation behavior of the drug-loaded hydrogel was further quantified by monitoring mass loss over 14 days. Under physiological conditions (PBS, pH 7.4, 37°C), the hydrogel displayed high structural stability, with only ~5% mass loss at day 14. In contrast, under accelerated alkaline conditions

(0.5 M NaOH, 37°C), the hydrogel underwent rapid degradation, with approximately 80% mass loss over the same period. These results confirm that the hydrogel is stable within the time window of *in vitro* experiments while remaining hydrolytically degradable under harsh conditions.

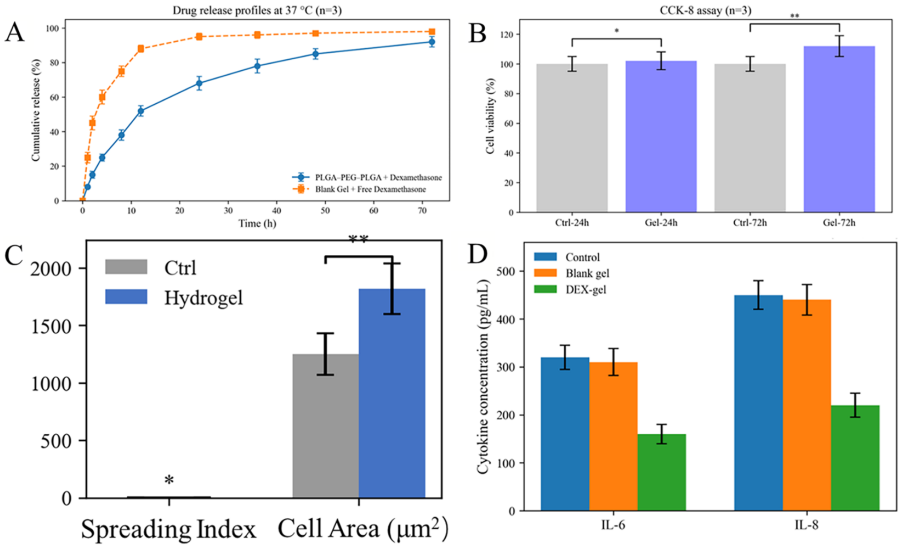

Figure 4. Biological evaluation of the PLGA–PEG–PLGA hydrogel system. (A) *In vitro* drug release profiles at 37°C (n = 3) comparing PLGA–PEG–PLGA hydrogel–encapsulated dexamethasone with blank gel containing free drug. (B) CCK-8 assay results showing relative cell viability after 24 and 72 h incubation. (C) Quantification of cytoskeletal morphology by spreading index and cell area. (D) ELISA measurements of pro-inflammatory cytokines (IL-6 and IL-8) after 24 h treatment with hydrogel. $p < 0.05$ (*), $p < 0.01$ (**)

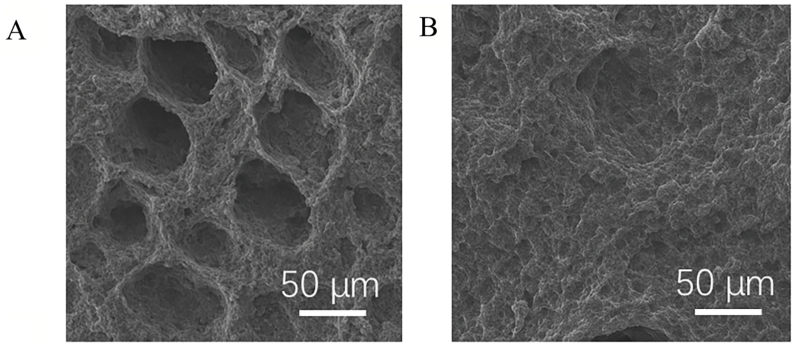

Figure 5. Continued

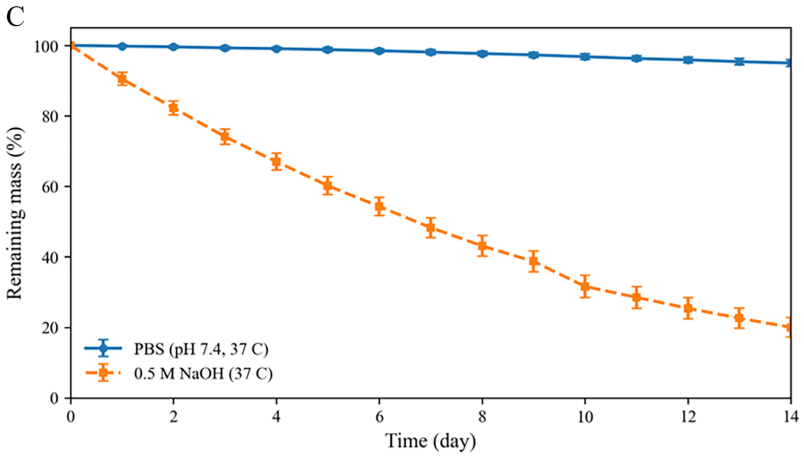

Figure 5. Microstructure and degradation behavior of the dexamethasone-loaded PLGA–PEG–PLGA hydrogel. (A) Representative SEM images show the porous network structure of the freeze-dried hydrogel before degradation. (B) After degradation treatment, the images reveal a denser, less porous morphology (right) (scale bar: 50 μm). (C) The degradation profiles of the drug-loaded hydrogel were evaluated under physiological conditions (PBS, pH 7.4, 37°C) and accelerated alkaline conditions (0.5 M NaOH, 37°C). Data are presented as mean ± SD (n = 3)

4. Discussion

As shown in Figure 1, the thermosensitive behavior of PLGA–PEG–PLGA is critical for its potential clinical application. The sol–gel transition allows the material to be injected as a liquid, minimizing patient discomfort and ensuring accurate delivery into the prostate. After injection, the *in situ* gelation provides a localized drug depot that reduces systemic exposure and increases drug retention time at the target site. This feature is particularly advantageous for chronic prostatitis treatment, where conventional oral or systemic administration often leads to fluctuating plasma concentrations and insufficient drug levels in the prostate [25]. The illustrated diffusion process further highlights the sustained release mechanism. Drug release is initially governed by diffusion through the micellar network, followed by gradual matrix relaxation, which prolongs the delivery period [26,27]. This dual-phase release behavior could help maintain therapeutic concentrations for an extended duration, potentially reducing dosing frequency. Moreover, the local delivery strategy reduces systemic side effects and improves drug bioavailability at the inflamed tissue. Taken together, the observations in Figure 1 provide strong evidence that the PLGA–PEG–PLGA hydrogel represents a promising platform for localized, controlled delivery of anti-inflammatory agents in prostatitis therapy. In the present system, dexamethasone is loaded into the PLGA–PEG–PLGA hydrogel mainly through hydrophobic association rather than specific covalent interactions. Dexamethasone is a relatively hydrophobic corticosteroid with low aqueous solubility, and thus preferentially partitions into the hydrophobic PLGA-rich domains of the amphiphilic triblock copolymer instead of the surrounding aqueous phase. Upon temperature-induced micellization and gelation, these PLGA cores become physically packed into a three-dimensional network, which further enhances drug retention and contributes to the sustained release behavior observed in our *in vitro* studies. This hydrophobic-core loading mechanism has been reported for dexamethasone and other hydrophobic drugs in PLGA–PEG–PLGA or related thermosensitive hydrogel systems, supporting the plausibility of the drug encapsulation mode proposed in this work [28]. Although the microstructure of the hydrogel was not directly visualized by SEM in this study, such imaging mainly reflects pore morphology and cannot unambiguously resolve drug distribution at the molecular level; therefore, we rely on the combination of polymer structure, drug physicochemical properties and

release profiles, together with previously reported PLGA–PEG–PLGA–based dexamethasone carriers, to rationalize the loading mechanism in our system.

As shown in Figure 2, the combined analytical results verify the structural fidelity and compositional accuracy of the synthesized PLGA–PEG–PLGA copolymer. The unimodal GPC profile suggests efficient ring-opening polymerization and minimal chain termination, while FTIR spectra confirm the coexistence of PEG ether linkages and PLGA ester groups [5]. Importantly, the ^{1}H NMR-derived ratios of PEG:LA and LA:GA closely align with design expectations, indicating reliable control over monomer incorporation during synthesis. Such consistency in molecular architecture is critical, as the hydrophilic–hydrophobic balance directly governs micelle formation, sol–gel transition temperature, and drug-loading capacity of the hydrogel system.

The results presented in Figure 3 confirm that the PLGA–PEG–PLGA copolymer exhibits the desired thermosensitive properties required for injectable hydrogel applications. The observed sol–gel transition around physiological temperature ensures convenient handling at low temperature and *in situ* gelation after administration. The rheological profiles underscore the balance between elasticity and viscosity, which is crucial for maintaining depot stability while still allowing diffusion-mediated drug release [29]. The injectability data highlight the translational potential of this system, as injection through 22–25 G needles required forces that are clinically manageable. Collectively, these findings emphasize that the hydrogel combines favorable thermal responsiveness, robust gel mechanics, and practical administration characteristics, making it a promising platform for localized prostate drug delivery.

The findings presented in Figure 4 highlight the multifunctional benefits of the PLGA–PEG–PLGA hydrogel as a localized drug delivery platform. The sustained release behavior of encapsulated dexamethasone prolongs therapeutic exposure, contrasting with the burst release of free drug and thereby offering the potential to reduce dosing frequency. The CCK-8 results suggest good cytocompatibility and even a supportive microenvironment for cell growth over extended culture. Enhanced spreading index and increased cell area imply that the hydrogel surface facilitates cytoskeletal reorganization, which is favorable for tissue integration. With the inclusion of the blank hydrogel group, the origin of the cytokine reduction can now be more clearly interpreted. The blank PLGA–PEG–PLGA hydrogel produced cytokine levels comparable to the untreated control, confirming that the hydrogel matrix does not inherently suppress inflammatory signaling in prostate epithelial cells. In contrast, the dexamethasone-loaded hydrogel significantly lowered IL-6 and IL-8 secretion, which is consistent with the known glucocorticoid-mediated inhibition of pro-inflammatory pathways. The difference between blank and drug-loaded hydrogels therefore verifies that the anti-inflammatory effects observed in this study are driven by dexamethasone release rather than by material-derived biological activity [29]. Collectively, these outcomes demonstrate that the hydrogel not only achieves controlled drug release but also exerts positive biological effects, reinforcing its translational potential for localized therapy. To further clarify the connection between physicochemical properties and the drug release behavior observed in this study, it is important to consider several structural features intrinsic to PLGA–PEG–PLGA hydrogels. Although only one copolymer composition was examined, the sol–gel transition temperature, rheological characteristics, and micelle-driven assembly collectively reflect the internal network architecture formed at physiological temperature. The transition from a free-flowing solution to a physically crosslinked gel indicates the formation of densely packed PLGA-rich hydrophobic domains, which act as diffusion barriers regulating dexamethasone transport. Because dexamethasone is a hydrophobic molecule, it preferentially partitions into these PLGA domains, resulting in a release profile dominated by diffusion through the micellar network and gradual relaxation of polymer chains. This mechanistic framework, supported by previous reports on PLGA–PEG–PLGA hydrogels, provides a reasonable explanation for the sustained release behavior observed in our formulation even in the absence of multiple structural variants. Thus, the existing characterization data already allow us to

articulate how the material's physicochemical features shape its release performance within the context of this cell-level study.

In the context of localized anti-inflammatory delivery, several alternative carriers—including liposomes, microgels, and nanoparticle-based depots—have been investigated for improved drug penetration into the prostate. Compared with these systems, the PLGA–PEG–PLGA hydrogel used in this study offers distinct practical advantages, such as temperature-triggered injectability, *in situ* gel formation, and the ability to accommodate hydrophobic drugs like dexamethasone without chemical modification. The sustained release behavior observed here suggests reduced burst release relative to some previously reported PLGA–PEG–PLGA formulations, which often suffer from rapid initial diffusion due to loosely packed micellar domains. The improved stability of the gel network at physiological temperature, together with its viscoelastic properties, provides a more controlled diffusion environment that may address limitations noted in earlier systems. Although our work remains at the *in vitro* stage, these characteristics underscore the potential of this formulation to complement or improve upon previously explored carrier technologies.

The SEM observations provide direct evidence of a well-defined porous network in the dexamethasone-loaded PLGA–PEG–PLGA hydrogel, which is essential for both mechanical integrity and diffusion-regulated drug release. Although SEM cannot resolve the molecular distribution of dexamethasone, the preserved network morphology supports the formation of a stable gel matrix capable of retaining hydrophobic drugs within PLGA-rich domains.

The degradation study further clarifies the relationship between hydrogel stability and drug release. The minimal mass loss observed in PBS indicates that degradation plays a negligible role during short-term cell experiments, suggesting that dexamethasone release under these conditions is primarily diffusion-controlled. Conversely, the rapid degradation under alkaline conditions confirms the hydrolytically labile nature of the PLGA segments and highlights the potential contribution of degradation to accelerated release at later stages. Together, these findings establish a clear distinction between diffusion-dominated release during *in vitro* evaluation and degradation-assisted release under aggressive conditions, addressing the coupling between degradation and drug release.

5. Conclusion

In conclusion, this study presents a systematic *in vitro* evaluation of a thermosensitive PLGA–PEG–PLGA hydrogel for sustained dexamethasone delivery in prostate epithelial cells. The hydrogel exhibited a well-defined porous network structure, favorable sol–gel transition behavior, and stable rheological properties. Degradation studies revealed high structural stability under physiological conditions and confirmed hydrolytic degradability under accelerated conditions, clarifying the interplay between degradation and drug release. The sustained release of dexamethasone effectively suppressed pro-inflammatory cytokine secretion without compromising cytocompatibility, while blank hydrogels showed no intrinsic anti-inflammatory activity. These findings demonstrate that the observed biological effects are primarily drug-driven and diffusion-dominated within the experimental timeframe. Although limited to *in vitro* evaluation, this work establishes a solid physicochemical and biological foundation for future studies exploring the *in vivo* performance and therapeutic potential of thermosensitive PLGA–PEG–PLGA hydrogels.

Acknowledgement: Not applicable.

Funding Statement: The study was supported by Capital's Funds for Health Improvement and Research (2022-2-7015).

Author Contributions: All authors contributed to this present work: [Chenglong Zheng] designed the study, [Huiqing Wu] acquired the data, [Hui Wang] interpreted the data. [Yue Lan] drafted and revised the manuscript. All authors reviewed and approved the final version of the manuscript.

Availability of Data and Materials: The datasets generated and/or analyzed during the current study are available from the corresponding author Yue Lan upon reasonable request.

Ethics Approval: Not applicable.

Conflicts of Interest: The authors declare no conflicts of interest.

Abbreviations

CCK-8	Cell Counting Kit-8
$CDCl_3$	Deuterated chloroform
CP/CPPS	Chronic prostatitis/chronic pelvic pain syndrome
DAPI	4′,6-diamidino-2-phenylindole
DMEM	Dulbecco's Modified Eagle Medium
DSC	Differential Scanning Calorimetry
ELISA	Enzyme-Linked Immunosorbent Assay
FBS	Fetal Bovine Serum
FITC	Fluorescein Isothiocyanate
FTIR	Fourier Transform Infrared Spectroscopy
GA	Glycolide
GPC	Gel Permeation Chromatography
G′ (Gp)	Storage modulus
G″ (Gpp)	Loss modulus
IL-6	Interleukin-6
IL-8	Interleukin-8
LA	L-lactide
NMR	Nuclear Magnetic Resonance
PBS	Phosphate-Buffered Saline
PEG	Poly(ethylene glycol)
PLGA	Poly(lactic-co-glycolic acid)
PLGA–PEG–PLGA	Poly(lactic-co-glycolic acid)–poly(ethylene glycol)–poly(lactic-co-glycolic acid)
RWPE-1	Human prostate epithelial cell line
$Sn(Oct)_2$	Stannous octoate
TMS	Tetramethylsilane
UV–vis	Ultraviolet–visible spectroscopy

References

1. Bastidas JG, Maurmann N, Oliveira L, Alcantara B, Pinheiro CV, Leipnitz G, et al. Bilayer scaffold from PLGA/fibrin electrospun membrane and fibrin hydrogel layer supports wound healing *in vivo*. Biomed Mater. 2023;18(2):025020. doi:10.1088/1748-605X/acb02f.
2. Fang W, Wang S, Dong JK, Zhang JY, Li XC, Fu CW, et al. Evaluation of clinical effect of acupuncture on chronic prostatitis: meta analysis. Am J Mens Health. 2025;19(1):15579883241290035. doi:10.1177/15579883241290035.
3. Borgert BJ, Wallen EM, Pham MN. Prostatitis a review. JAMA. 2025;334(11):1003–13. doi:10.1001/jama.2025.11499.
4. Cesta N, Fusco A, Ferretti C, Materazzi A, Altieri A, D'Agostini C, et al. Bacteriophage-enhanced doxycycline activity against *Escherichia coli* in chronic bacterial prostatitis. Int J Antimicrob Agents. 2025;66(4):107571. doi:10.1016/j.ijantimicag.2025.107571.

5. Zhang J, Qiao J, Zhang Y, Zhu H, Haubruge E, Liu L, et al. Di-p-coumaroyl spermidine from bee pollen alleviates chronic nonbacterial prostatitis. Food Sci Nutr. 2025;13(6):e70467. doi:10.1002/fsn3.70467.
6. Hua L, Gao X, Zhan J, Wu X, Liu H. Prostatitis and male infertility. Aging Male. 2025;28(1):2494550. doi:10.1080/13685538.2025.2494550.
7. Ma X, Lao Y, Bai Y, Guan X, Jiang J, Cui M, et al. Study progress of etiologic mechanisms of chronic prostatitis/chronic pelvic pain syndrome. Int Immunopharmacol. 2025;148(3):114128. doi:10.1016/j.intimp.2025.114128.
8. Kadlecová Z, Sevriugina V, Lysáková K, Rychetský M, Chamradová I, Vojtová L. Liposomes affect protein release and stability of ITA-modified PLGA-PEG-PLGA hydrogel carriers for controlled drug delivery. Biomacromolecules. 2024;25(1):67–76. doi:10.1021/acs.biomac.3c00736.
9. Folle C, Díaz-Garrido N, Mallandrich M, Suñer-Carbó J, Sánchez-López E, Halbaut L, et al. Hydrogel of thyme-oil-PLGA nanoparticles designed for skin inflammation treatment. Gels. 2024;10(2):149. doi:10.3390/gels10020149.
10. Lysakova K, Hlinakova K, Kutalkova K, Chaloupkova R, Zidek J, Brtnikova J, et al. Novel approach in control release monitoring of protein-based bioactive substances from injectable PLGA-PEG-PLGA hydrogel. Express Polym Lett. 2022;16(8):798–811. doi:10.3144/expresspolymlett.2022.59.
11. Li B, An T, Song D, Lu X, Huo Y, Chu Y, et al. Dominant role of distinct microenvironments on cartilage regeneration fate using PLGA-hydrogel composite scaffolds. Adv Healthc Mater. 2025;14(12):e2405272. doi:10.1002/adhm.202405272.
12. Lefol LA, Bawuah P, Zeitler JA, Verin J, Danede F, Willart JF, et al. Drug release from PLGA microparticles can be slowed down by a surrounding hydrogel. Int J Pharm X. 2023;6(3):100220. doi:10.1016/j.ijpx.2023.100220.
13. Kontogiannis DS, Agoranou ME, Dimitriadis F, Skouteris VM, Falagas ME. Fosfomycin for the treatment of patients with bacterial prostatitis: a systematic review. Eur J Clin Microbiol Infect Dis. 2025;44(8):1835–48. doi:10.1007/s10096-025-05173-x.
14. Folle C, Marqués AM, Mallandrich M, Suñer-Carbó J, Halbaut L, Sánchez-López E, et al. Colloidal hydrogel systems of thymol-loaded PLGA nanoparticles designed for acne treatment. Colloids Surf B Biointerfaces. 2024;234(1):113678. doi:10.1016/j.colsurfb.2023.113678.
15. Piao L, Xiang P, Zhou Y, Zhao W, Yang T, Xia S, et al. Thermo-sensitive PLGA-PEG-PLGA hydrogel for sustained release of EGF to inhibit cervical cancer recurrence. Colloids Surf B Biointerfaces. 2024;236:113795. doi:10.1016/j.colsurfb.2024.113795.
16. Gu W, Fan R, Quan J, Cheng Y, Wang S, Zhang H, et al. Intracranial *in situ* thermosensitive hydrogel delivery of temozolomide accomplished by PLGA-PEG-PLGA triblock copolymer blending for GBM treatment. Polymers. 2022;14(16):3368. doi:10.3390/polym14163368.
17. Meng T, Zhang Y, Wang H, Wu W, Peng W, Yue J, et al. Irf7 aggravates prostatitis by promoting Hif-1α-mediated glycolysis to facilitate M1 polarization. Cell Mol Life Sci. 2025;82(1):90. doi:10.1007/s00018-025-05608-w.
18. Manhas P, Sharma R, Wangoo N, Saini R, Saima, Agrewala JN, et al. Dox-loaded TPU-PLGA nanoparticles embedded chitosan hydrogel formulation as an effective anti-cancer therapy. J Mol Liq. 2023;383(4):122170. doi:10.1016/j.molliq.2023.122170.
19. Heine S, Aguilar-Pimentel A, Russkamp D, Alessandrini F, Gailus-Durner V, Fuchs H, et al. Thermosensitive PLGA-PEG-PLGA hydrogel as depot matrix for allergen-specific immunotherapy. Pharmaceutics. 2022;14(8):1527. doi:10.3390/pharmaceutics14081527.
20. He X, Liu D, Cui B, Huang H, Dai S, Pang I, et al. Extreme hydrogel bioelectronics. Adv Funct Mater. 2024;34(52):2405896. doi:10.1002/adfm.202405896.

21. Wang Y, Ji H, Chen Y, Zhu B, Peng Y, Xing Q. The negative feedback of the glutamine/prostatitis loop identified among 1400 metabolites and prostatitis via Mendelian randomization. Mediators Inflamm. 2025;2025(1):9648279. doi:10.1155/mi/9648279.
22. Woodard TJ, Ransom CD, Kim D, Razzaq T. The pharmacist's guide to acute bacterial prostatitis. US Pharm. 2025;50(6):12–6. doi:10.18591/bjuik.0058.
23. Tsai LH, Young TH, Yen CH, Yao WC, Chang CH. Intratumoral thermo-chemotherapeutic alginate hydrogel containing doxorubicin loaded PLGA nanoparticle and heating agent. Int J Biol Macromol. 2023;251:126221. doi:10.1016/j.ijbiomac.2023.126221.
24. Rahmani F, Atabaki R, Behrouzi S, Mohamadpour F, Kamali H. The recent advancement in the PLGA-based thermo-sensitive hydrogel for smart drug delivery. Int J Pharm. 2023;631(2):122484. doi:10.1016/j.ijpharm.2022.122484.
25. Yuan B, Zhang Y, Wang Q, Ren G, Wang Y, Zhou S, et al. Thermosensitive vancomycin@PLGA-PEG-PLGA/HA hydrogel as an all-in-one treatment for osteomyelitis. Int J Pharm. 2022;627:122225. doi:10.1016/j.ijpharm.2022.122225.
26. Yan K, Tao Y, Chen B, Zhang D, Li Z, Li C, et al. Identifying causal genes for prostatitis through drug-targeted Mendelian randomization. Sci Rep. 2025;15(1):19069. doi:10.1038/s41598-025-03510-w.
27. Khodaverdi E, Kheirandish F, Mirzazadeh Tekie FS, Khashyarmanesh BZ, Hadizadeh F, Moallemzadeh Haghighi H. Preparation of a sustained release drug delivery system for dexamethasone by a thermosensitive, *in situ* forming hydrogel for use in differentiation of dental pulp. ISRN Pharm. 2013;2013(1):983053. doi:10.1155/2013/983053.
28. Zhao HY, Jiang JB, Chen Y, Miao CY. The hMetrnl-PLGA-PEG-PLGA hydrogel facilitates skin wound healing through dual regulation on *ENOS* activity and stability. Pharmaceuticals. 2025;18(8):1180. doi:10.3390/ph18081180.
29. Zhou J, Ding L, Chen J, Chen C, Jiang P, Mei Z, et al. HMGB1 inhibition alleviates chronic nonbacterial prostatitis by suppressing M1 polarization of macrophages. J Inflamm Res. 2025;18:6735–48. doi:10.2147/JIR.S502616.

Received: 22 September 2025; Accepted: 08 January 2026; Published: xx xxx 2026